Initiation of air ionization by ultrashort laser pulses: Evidence for a role of metastable-state air molecules

Initiation of air ionization by ultrashort laser pulses: Evidence for a role of metastable-state air molecules

A. V. Bulgakov[1,2,a)], **I. Mirza**[1], **N. M. Bulgakova**[1,2], **V. P. Zhukov**[1,3,4], **R. Machulka**[5], **O. Haderka**[5], **E. E. B. Campbell**[6,7] **and T. Mocek**[1]

[1] HiLASE Centre, Institute of Physics of the Czech Academy of Sciences, Za Radnicí 828, 25241 Dolní Břežany, Czech Republic

[2] S.S. Kutateladze Institute of Thermophysics SB RAS, Lavrentyev Ave. 1, Novosibirsk 630090, Russia

[3] Institute of Computational Technologies SB RAS, 6 Lavrentyev Ave., 630090 Novosibirsk, Russia

[4] Novosibirsk State Technical University, 20 Karl Marx Ave., 630073, Novosibirsk, Russia

[5] Joint Laboratory of Optics of Palacký University and Institute of Physics of the Czech Academy of Sciences, Palacký University, Listopadu 12, 77146 Olomouc, Czech Republic

[6] EaStCHEM, School of Chemistry, University of Edinburgh, Edinburgh EH9 3FJ, UK

[7] Division of Quantum Phases and Devices, School of Physics, Konkuk University, Seoul, 143-701 South Korea

[a] Author to whom correspondence should be addressed

E-mail: bulgakov@fzu.cz and bulgakov@itp.nsc.ru

Abstract

Transmission measurements for femtosecond laser pulses focused in air with spectral analysis of emission from the focal region have been carried out for various pulse energies and air pressures. The air breakdown threshold and pulse attenuation due to plasma absorption are evaluated and compared with calculations based on the multiphoton ionization model. The plasma absorption is found to depend on the pulse repetition rate and is considerably stronger at 1 kHz than at 1-10 Hz. This suggests that accumulation of metastable states of air molecules plays an important role in initiation of air breakdown, enhancing the ionization efficiency at high repetition rates. Possible

channels of metastable-state-assisted air ionization and the role of the observed accumulation effect in laser material processing are discussed.

Keywords: femtosecond laser pulses, laser-induced air breakdown, multiphoton ionization, metastable-state molecules

1. Introduction

Interaction of ultrashort laser pulses with gases provides a basis for a number of fascinating non-linear phenomena, for instance generation of high-order harmonics [1], attosecond pulses [2], terahertz radiation [3] and lasing actions [4,5], and is of crucial importance in laser-material processing. The vast majority of scientific and technological applications of short and ultrashort laser processing of materials are performed in a gas environment, mainly in air under atmospheric conditions. However, the role of ambient gases is so far insufficiently understood due to the complexity of laser beam propagation in ionizable media and the large variety of involved processes. It has been shown that the presence of a gas environment can lead to higher target absorptivity [6], ultra-deep crater formation [7,8], alterations in non-equilibrium surface conditions [9], and can cause misinterpretation of laser ablation mechanisms [10].

When a femtosecond laser pulse propagates in air, many nonlinear optical effects, such as multiphoton ionization (MPI), tunnel ionization, optical Kerr effect, Raman scattering, white-light generation, and conical off-axis emission, come into play to induce air breakdown, thus affecting the pulse properties [11-14]. The formation of laser-induced filaments, enabling the beam to propagate over extended distances is mainly due to the competitive action of MPI and self-focusing governed by the Kerr effect [12]. In laser processing experiments under tightly focused conditions when the role of self-focusing is minimized [15], MPI processes play the main role in initiating the air breakdown [11].

In ultrashort pulse laser processing, high-repetition rate lasers (in the range of kHz and even MHz) are often used to increase the processing efficiency. This can result in accumulation of the laser energy in the ambient gas if the repetition rate exceeds the rates of heat or excitation dissipation. While various accumulation effects, such as laser-induced formation of defect states and morphological changes on material surfaces and in volume, have widely been studied [9,16-

19], little attention is paid to the fact that excited molecular and atomic states and hydrodynamic perturbations in ambient gases can also be accumulated, thus facilitating gas ionization by subsequent laser pulses. However, there is evidence to indicate that long-lived non-equilibrium conditions can occur in air after propagation of an intense laser pulse. For instance, preliminary laser excitation of the atmospheric air increases considerably the efficiency of third harmonic generation at 10 μs timescale delays suggesting an important role of metastable neutrals [20]. The well-known phenomenon of a short-lived afterglow, or pink afterglow, occurring for about 1-10 ms after a discharge in N_2, also implies that metastable nitrogen molecules are responsible for the emission in the pink region [21-24]. In addition, calculations [6,8] show that, after recombination of the fs-laser-induced breakdown plasma on a nanosecond timescale, the perturbed gas is hot, initiating hydrodynamic motion with complicated shock-wave structures for long times up to ~ 100 μs.

In this Letter we report experimental evidence for an accumulation effect during propagation of femtosecond laser pulses in air based on optical transmission measurements, spectral analysis of the emission from the focal region and theoretical analysis of air ionization. The results confirm the role of metastable states of air molecules in initiation of air breakdown, enhancing the ionization efficiency at high laser repetition rates.

2. Experimental

The 800 nm, 120 fs output from a Ti:sapphire laser with pulse energy up to 1 mJ was used in the measurements. A scheme of the experimental setup is shown in Fig. 1. The laser pulses were focused by a lens (focal distance 25 or 20 cm) into a vacuum chamber (background pressure below 10^{-6} mbar) where the air pressure was varied in the range 0.1 – 1 bar. The experiments were performed for three laser repetition rates, 1, 10 and 1000 Hz, which were obtained by changing the configuration of a pulse picker. Particular attention was paid to measuring the focus beam waist w_0 (i.e., $1/e^2$-radius of the beam radial intensity distribution) in order to accurately determine the laser fluence in the focus. For this purpose, a series of ablation experiments with targets (silicon wafers, polished gold) placed in the focal region was performed. The laser-induced damage area was measured as a function of pulse energy and the w_0 value was determined using the D^2 – method for Gaussian beams [25,26]. The measurements were performed in the focal region for several

distances from the lens that provided us with the exact position of the focus. The determined w_0 values were 20.2 ± 0.5 μm for the 20-cm focal lens and 25.3 ± 0.5 μm for the 25-cm focal lens. The beam waist was measured for 1, 10 and 1000 Hz and identical results were obtained suggesting the same beam quality for the three repetition rates investigated. The pulse energy E_0 was adjusted using a λ/2 plate in combination with a Glan polarizer to give a peak laser fluence $F_0 = 2E_0/\pi w_0^2$ in the range 2-80 J/cm^2.

A small central part of the outgoing diverging beam was selected at 25 cm from the focus using a 0.2 mm diameter aperture and split into two portions by a glass plate. The reflected low-intensity portion was detected using a fast photodiode with an optical filter in front of it and monitored on a digital oscilloscope. The time-integrated photodiode signal was calibrated as a function of the incident pulse energy in the absence of any absorption effects under vacuum conditions. In the experiment we used either a narrow bandpass interference filter (800 nm central wavelength, 10 nm FWHM) or a longpass filter (> 600 nm) and obtained identical results that indicated negligible spectral broadening of the incident radiation observed for higher laser intensities [10,12,25]. Note that the used experimental scheme with analysis of the transmission of the central beam fraction is more sensitive to plasma initiation than measuring the total transmitted pulse energy, especially near the air breakdown threshold, due to stronger attenuation of the most intense central part of the beam [6,8,28,29]. The time-integrated spectra of the emission from the focal region were investigated using an Ocean Optics fiber spectrometer (200-1000 nm spectral range, 0.4 nm resolution) with the fiber tip placed near the focus, a few mm away from the beam axis (Fig. 1). The spectra were averaged over 20,000 – 50,000 laser shots and the background was subtracted.

3. Modeling

Theoretical analysis of the laser-induced air ionization and beam propagation under the experimental conditions was based on the geometrical optics model taking into account the radiation attenuation due to photoionization. The model was developed in Ref. 11 to gain insight into dynamics of air ionization by fs laser pulses in front of metallic targets incorporating the interference effect of the incoming and reflected light. In this study, we have modified the model for the case of light propagation in air in the absence of a target.

The laser beam focusing is described by the geometrical optics for Gaussian laser beams. Under such an approach, the trajectory radius of a beam ray $r(\rho,z)$, which propagates along the z direction and crosses the focal plane (located at $z = 0$) at a radius ρ from the beam axis, can be expressed as $r = s^{0.5}\rho$ where $s(z) = 1 + z^2/z_R^2$ and z_R is the Rayleigh length. The simulations start when the beam is at a distance $z = -z_0$ from the geometrical focus, which is large enough to ensure the absence of gas ionization at this distance. The incoming laser light flux ε is expressed as follows:

$$\varepsilon = \frac{F_0 \exp(-r^2/w_0^2 - t^2/t_L^2)}{\sqrt{\pi} t_L c_z s(-z_0)}. \quad (1)$$

Here $t_L = \tau/(2\sqrt{\ln 2})$ with laser pulse duration (FWHM) τ = 120 fs; $c^2 = c_z^2 + c_r^2$ is the velocity of light; $c_z = c/[1 + (\partial r/\partial z)^2]$. Then, the following equation can be written for the beam propagation:

$$\frac{\partial \varepsilon}{\partial t} + \frac{1}{r}\frac{\partial (r c_r \varepsilon)}{\partial r} + \frac{\partial (c_z \varepsilon)}{\partial z} = -Q \quad (2)$$

where Q accounts for the losses of laser energy. Taking into account that, for ultrashort laser pulses, the laser light is absorbed by the ambient gas only via photoionization and involving the beam trajectory formalism presented above, one can write:

$$\frac{\partial s\varepsilon}{\partial t} + \frac{\partial (s c_z \varepsilon)}{\partial z} = -s W_{PI} k \hbar \omega. \quad (3)$$

For simplicity, we consider only multiphoton ionization (MPI) with $W_{PI} = AI^k (n_0 - n_e)/n_0$ where $I = I(z,t) = c\varepsilon$ is the local laser intensity, k is the order of photoionization, and n_0 is the initial density of the ambient gas molecules which may be considered unchanged during fs laser irradiation. Simulations are performed for nitrogen as the main constituent of air with k = 11 for the wavelength of 800 nm and the MPI coefficient A adapted from [30]. Note that, at high laser intensities, the tunnel ionization (TI) mechanism, discussed below, can dominate [11,12]. As we are interested merely in the time associated with the laser pulse propagation, collisional ionization and plasma recombination are disregarded as they occur later [8,11].

4. Results and discussion

Figure 2 shows the transmitted pulse energy of the central beam fraction as a function of the incident laser fluence in ambient air and in high vacuum for the 20 cm lens. There is no beam attenuation in vacuum and thus the transmission dependence is perfectly linear. In air, a clearly defined deviation from the linear dependence is seen starting from a threshold fluence of ~26 J/cm^2 (2.1×10^{14} W/cm^2). This is due to the well-known effect of air ionization by laser pulses (air breakdown) and the corresponding laser energy losses [8,11,12,31-33]. The threshold value agrees with the available thresholds for fs-laser air breakdown reported in the range (1-3) $\times 10^{14}$ W/cm^2 [31-33]. However, transmission measurements for the *total pulse energy* provide considerably higher threshold values, by a factor of 2 to 3 [33,34].

Interestingly, for the 25 cm lens the results are very similar. At first glance, for the same peak intensity the longer-focus lens provides a longer ionization region according to the geometrical optics of Gaussian beams. Hence, the laser beam depletion should be stronger than for the 20 cm lens. However, as our simulations show, the maximum ionization degree is higher for shorter-focus lenses due to faster narrowing the cross section of the laser beam upon its approaching the focal plane. A similar effect of increased ionization for higher numerical apertures was observed previously for fs-laser pulse propagation in fused silica [35]. This effect of increased ionization for the 20-cm lens compensates the longer ionization distance for the 25-cm lens and thus results in similar pulse energy losses. For even shorter focal lengths, this compensation may not be achieved and will require further studies for quantification.

Near and slightly above the fs breakdown threshold, MPI is believed to play a major role in the ionization process [8,11,12,28,32]. This is supported by our MPI-based model calculations which predict accurately the threshold fluence for the beam attenuation in air for the experimental conditions (figure 2). With further increase in fluence, the calculations somewhat overestimate the energy losses probably due to the onset of TI in this fluence region, thus affecting the photoionization process [11,12]. The transition between MPI and TI regimes is controlled by the Keldysh parameter $\gamma = \omega(2mI_0)^{1/2}/(eE_0)$, where ω and E_0 are the frequency and strength of the laser electric field, I_0 is the ionization potential, and e and m are the electron charge and mass, with conditions $\gamma >> 1$ and $\gamma << 1$ correspond to the MPI and TI regimes, respectively [36]. A detailed analysis of ultrashort pulse laser ionization experiments revealed [11] that TI dominates at $\gamma < 0.5$ whereas in the transition region of $\gamma = 0.5$-1 (corresponding to the fluence range of 18-70 J/cm^2 in vacuum for our laser pulses, the most interesting region for our experiments, see figure 2), MPI

still contributes significantly at the rising/falling parts of the pulse. In addition, the laser intensity clamping effect (see Refs. 8 and 28 and discussion below) reduces the maximum intensity reached upon the laser beam propagation and further increases the contribution of MPI. Note also that the critical laser power P_{cr} for self-focusing of 800-nm pulses in air is [12] P_{cr} = 3.2 GW that corresponds to a laser fluence of 62 J/cm^2 for our experimental conditions and is considerably larger than the observed breakdown threshold (figure 2).

The most remarkable feature of the results in figure 2 is the dependence of the transmitted energy on the laser repetition rate. The laser light transmission at 1 kHz is systematically lower than that at 10 Hz. This is particularly pronounced at fairly high fluences, above ~ 40 J/cm^2, when the 1 kHz signal is lower by 15-20 %. The transmitted signals at 10 Hz and 1 Hz are, however, nearly identical (figure 2). This indicates that non-equilibrium conditions with a lifetime in the range 1-100 ms are produced in air due to propagation of above-ionization-threshold laser pulses. Three possible processes can be conjectured for such long-lived phenomena in the gas phase, namely, plasma effects, hydrodynamic perturbations in the focal region, and generation of metastable molecules. The first process can be ruled out since the plasma decays on the time scale of several nanoseconds [31]. The hydrodynamic effects can also be excluded because strong shock-wave perturbations in air occur during ~ 100 μs under the experimental conditions and on longer timescales there is only slow air motion [6]. One could expect long-lasting variations of the air density due to an oscillating character of the hydrodynamic air motion similar to that observed in laser-induced plumes expanding into a background gas [37,38]. However, since the amplitude and period of such oscillations depend on the air pressure, this would manifest itself as a non-monotonic pressure dependence of the transmitted energy and that is not the case. Figure 3 shows the transmission signal measured at 1 and 1000 Hz as a function of the air pressure. The signal monotonically increases as the pressure is reduced with the difference of 1Hz and 1 kHz transmissions remaining unchanged in the pressure range of 0.2-1 bar. This indicates that the air oscillating motion, if it occurs, decays by the 1-ms timescale. Therefore, laser-produced metastable air molecules appear to be the most convincing explanation for the observed dependence on repetition rate.

Possible involved excitation-decay channels of laser-irradiated air molecules can be identified based on the recorded emission spectra (a typical spectrum is shown in figure 4(a)). The intensities of some representative lines are plotted in figure 4(b) as a function of input laser fluence. As seen, the main emission is observed from the N_2 2nd positive system (PS) $C^3\Pi_u - B^3\Pi_g$

which is detected at fluences well below the breakdown threshold. Weaker emission is registered from the N_2^+ 1st negative system (NS) $B^2\Sigma_u^+ - X^2\Sigma_g^+$, N_2 1st PS $B^3\Pi_g - A^3\Sigma_u^+$ and also from excited N and O atoms. The same bands were observed under fs-laser filamentation in air [4,5,29] and nitrogen [28] and in the pink afterglow [21-24] (although in the pink afterglow the intensity distribution between the bands is different and the N_2 2nd PS is relatively weak). No continuum radiation from the focal region is detected, indicating a negligible role of plasma recombination in the observed emission. The excitation of the N_2^+ $B^2\Sigma_u^+$ state is shown to be due to a direct MPI process and the intensity of the 1st NS emission is proportional to the total number of ions [28,29]. The mechanism of populating the $C^3\Pi_u$ state of N_2, which radiates in the dominating band, is not yet unambiguously determined. This can be either multiphoton excitation [39] or depopulation of some highly excited electronic states through collisions [29].

The $A^3\Sigma_u^+$ state of N_2, the lowest excited state with an excitation energy of 6.2 eV, is metastable with a radiative lifetime of about 2 s [20,40]. Its quenching occurs mainly through collisions with a rate of $\sim 3\times10^{-19}$ cm^3s^{-1} that corresponds to a decay time of about 100 ms under normal conditions [39,41]. Since the de-activation probability increases with temperature [40] and due to the presence of oxygen [41] we expect the quenching time for the N_2 $A^3\Sigma_u^+$ state in the focal region to be on the order of 10 ms. For instance, at 1000 K, a temperature easily reachable in air under the considered conditions [8], the average number of molecular collisions to de-activate the N_2 $A^3\Sigma_u^+$ state was found to be $\sim 5\times10^7$ [40] that gives us a decay time of ~ 20 ms at 1 bar (assuming nitrogen collisions with a gas kinetic cross section of 4×10^{-15} cm^2). This provides a convincing explanation for our observations. The ionization probability of this non-radiative excited state approaches 100% under our laser fluences [39] and thus the air ionization is enhanced in multi-pulse irradiation regimes if the pulse repetition rate is high enough (a few 100 Hz or more) to facilitate the breakdown initiation. It cannot be excluded that other long-lived excited states of air species like O ^1S (radiative lifetime 0.7 s), N $^2P^0$ (12 s) or O_2 $b^1\Sigma_g^+$ (7 s) are also involved in this process.

For all the observed emission lines, the emission intensity initially shows a quick increase with laser fluence before an abrupt change of the slope towards a slower increase at a fluence corresponding to the air breakdown threshold (figure 4(b)). This change of slope cannot be explained, for our high-pressure conditions, by the MPI-induced depletion of neutral molecules in the focal region but is due to a flattening of the pulse spatial profile during propagation (intensity

clamping) [28]. Figure 5 shows the calculated laser pulse profiles $I(r)$ after attenuation for difference input fluences. To calculate this, we assumed that the off-axis rays of our Gaussian beam are attenuated in the same way as its central portion (figure 2) according to the local incident intensity $I_0(r)$. The central part of the pulse experiences the strongest attenuation while the total transmitted energy is affected to a lesser extent for the considered fluence range. For instance, at 45 J/cm^2 the beam attenuation at the axis is 64% while 88% of the total incident energy is transmitted.

The observed accumulation effect can be even more pronounced for higher laser repetition rates (> 10 kHz), in particular for burst-mode lasers, when excited air molecules with shorter lifetimes can contribute to the initiation of air breakdown. These can be, for instance, $^1\Pi$ states of molecular nitrogen (~ 100 μs lifetime) responsible for the pink afterglow [21,42] or, as observed here, the N_2 $B^3\Pi_g$ state (~ 10 μs lifetime). Metastable-state-assisted laser-induced air ionization can be important for material processing by high-repetition-rate lasers imposing limitations on the achievable peak fluence at the processed surface due to the defocusing and clamping effects, thus strongly affecting the processing quality.

5. Conclusions

In this study, an accumulation effect during propagation of femtosecond laser pulses focused in air is observed for the first time using optical transmission measurements. The plasma absorption effects are found to depend on the pulse repetition rate and are considerably stronger at 1 kHz than at 1-10 Hz in a wide pressure range. The air breakdown threshold and pulse attenuation due to plasma absorption are evaluated and compared with calculations based on the multiphoton ionization model. Based on a spectral analysis of air plasma emission from the focal region, we demonstrate that metastable-states of air molecules play an important role in initiation of laser-induced air breakdown, enhancing the ionization efficiency at high laser repetition rates. The observed accumulation effect is important for material processing by high-repetition-rate lasers in air, in particular by burst-mode lasers, since it imposes limitations on the achievable laser fluence on the processed surface and results in a transformation of the laser spatial profile. Further work aimed at clarifying the channels of metastable-state-assisted laser-induced air ionization and its influence on the material processing quality is currently under way.

Acknowledgments

This work was co-financed by the European Regional Development Fund and the state budget of the Czech Republic (project BIATRI: No. CZ.02.1.01/0.0/0.0/15_003/0000445, project HiLASE CoE: No. CZ.02.1.010.00.015 0060000674, programme NPU I: project No. LO1602). AVB also acknowledges partial financial support from FASO Russia (project 22.8.2).

References

[1] L'Huiller A and Balcou P 1999 *Phys. Rev. Lett.* **70** 774

[2] Constant E, Garzella D, Breger P, Mevel E, Dorrer Ch, Le Blanc C, Salin F and Agostini P 1999 *Phys. Rev. Lett*. **82** 1668

[3] Kim K Y, Taylor A J, Glownia J H and Rodrigez G 2008 *Nature Photon*. **2** 605

[4] Luo Q, Liu W and Chin S I 2003 *Appl. Phys. B* **76** 337

[5] Yao J, Zheng B, Xu H, Li G, Chu W, Ni J, Zhang H, Chin S L, Cheng Y and Xu Z 2011 *Phys. Rev A* **84** 051802(R)

[6] Bulgakova N M, Zhukov V P, Vorobyev A Y and Guo C 2008 *Appl. Phys. A* **92** 883

[7] Bulgakova N M, Evtushenko A B, Shukhov Y G, Kudryashov S I and Bulgakov A V 2011 *Appl. Surf. Sci.* **257** 10876

[8] Bulgakova N M, Panchenko A N, Zhukov V P, Kudryashov S I, Pereira A, Marine W, Mocek T and Bulgakov A V 2014 *Micromachines* **5** 1344

[9] Gamaly E G, Madsen N R, Duering M, Rode A V, Kolev V Z and Luther-Davies B 2005 *Phys. Rev. B* **71** 174405

[10] Bulgakova N M and Bulgakov A V 2008 *Phys. Rev. Lett.* **101** 099701

[11] Chin S L 2004 *From Multiphoton to Tunnel Ionization* (Singapore, World Scientific)

[12] Couairon A and Mysyrowicz A 2007 *Phys. Rep.* **441** 47

[13] Broun A, Korn G, Liu X, Du D, Squier J and Mourou G 1995 *Opt. Lett.* **20** 73

[14] Klimentov S M, Kononenko T V, Pivovarov P A, Garnov S V, Konov V I, Breitling D and Dausinger F 2003 *Proc. SPIE* **5121** 77

[15] Heins A, Singh S C and Guo C 2017 *Phys. Plasmas* **24** 072101

[16] Eaton S M, Zhang H, Herman P R, Yoshino F, Shah L, Bovatsek J and Arai A Y 2005 *Opt. Express* **13** 4708

[17] Raciukaitis G, Brikas M, Gecys P and Gedvilas M 2008 *Proc. SPIE* **7005** 70052L

[18] Biswas S, Karthikeyan A and Kietzig A-M 2016 *Materials* **9** 1023

[19] Gill R K, Smith Z J, Lee C and Wachsmann-Hogiu S 2016 *J. Biophotonics* **9** 171

[20] Fedotov A B, Naumov A N, Silin V P, Uryupin S A, Zheltikov A M, Tarasevitch A P and von der Linde D 2000 *Phys. Lett. A* **271** 407

[21] Beale Jr. G E and Broida H P 1959 *J. Chem. Phys.* **31** 1030

[22] Lund R E and Oskam H J 1969 *Z. Physik* **219** 131

[23] Supiot P, Dessaux O and Goudmand P 1995 *J. Phys. D* **28** 1826

[24] Amorim J 2005 *IEEE Trans. Plasma Sci.* **33** 368

[25] Liu J M 1982 *Opt. Lett.* **7** 196

[26] Starinskiy S V, Shukhov Y G and Bulgakov A V 2017 *Appl. Surf. Sci.* **396** 1765

[27] Kasparian J, Sauerbrey R, Mondelain D, Niedermeier S, Yu J, Wolf J-P, André Y-B, Franco M, Prade B, Tzortzakis S, Mysirowicz A, Rodroges M, Wille H and Wöste L 2000 *Opt. Lett.* **25** 1397

[28] Becker A, Aközbek A, Vijayalakshmi K, Oral E, Bowden C M and Chin S L 2001 *Appl. Phys. B* **73** 287

[29] Talebpour A, Petit S and Chin S L 1999 *Opt. Commun.* **171** 285

[30] Couairon A and Bergé L. 2002 *Phys. Rev. Lett*. **88** 135003

[31] Martirosyan A E, Altucci C, Bruno A, de Lisio C, Porzio A and Solimeno S 2004 *J. Appl. Phys.* **96** 5450

[32] Bukin V V, Garnov S V, Malyutin A A and Strelkov V V 2007 *Quantum Electron.* **37**, 961

[33] Hu W, Shin Y C and King G 2011 *Appl. Phys. Lett.* **99** 234104

[34] Klimentov S M, Kononenko T V, Pivovarov P A, Garnov S V, Konov V I, Prokhorov A M, Breitling D and Dausinger F 2001 *Quantum Electron.* **31** 378

[35] Bulgakova N M, Zhukov V P, Sonina S V and Meshcheryakov Y P 2015 *J. Appl. Phys*. **118** 233108

[36] Keldysh L V 1965 *Sov. Phys. JETP* **20** 1307

[37] Bulgakov A V and Bulgakova N M 1995 *J. Phys. D* **28** 1710

[38] Bulgakov A V, Predtechensky M R and Mayorov A P *Appl. Surf. Sci.* **96-98** 159

[39] Xie H, Li G, Yao J, Chu W, Li Z, Zeng B, Wang Z and Cheng Y 2015 *Sci. Rep.* **5** 16006

[40] Haque R and von Engel A 1974 *Int. J. Electronics* **36** 239

[41] Hunten D M and McElroy M B 1966 *Rev. Geophys.* **4** 303

[42] Borst W L and Zipf E C 1971 *Phys. Rev. A* **3** 979

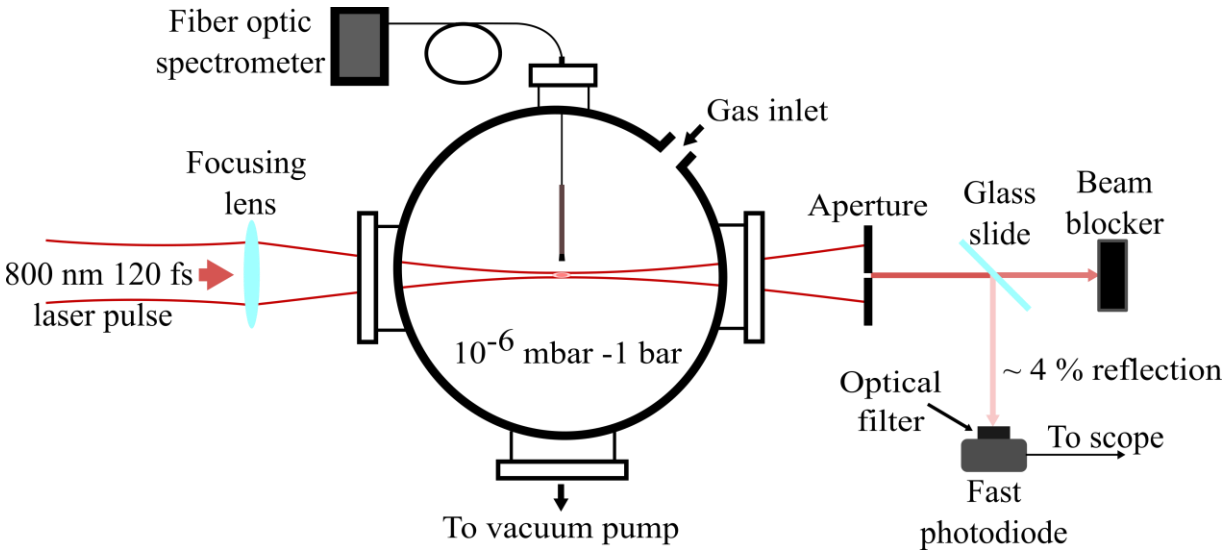

Figure 1. Experimental setup.

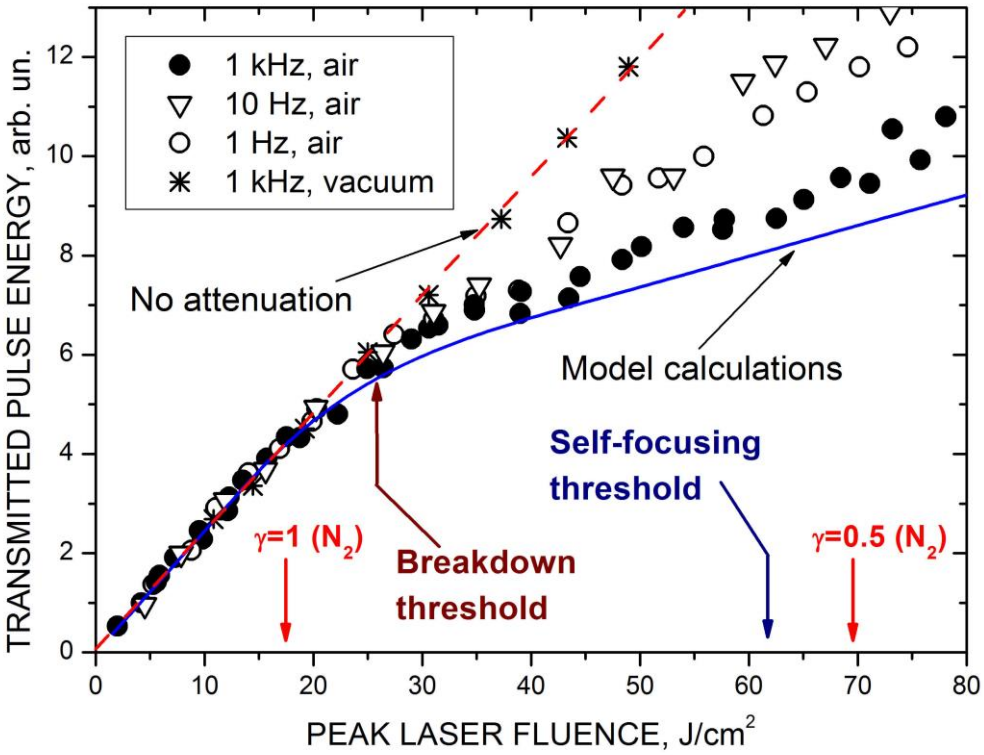

Figure 2. Measured (points) and calculated (solid line) transmitted laser pulse energy as a function of incident laser fluence at the focus (determined for conditions of no attenuation). The measurements were performed in vacuum and in 1 bar air at 3 different laser repetition rates with a 20-cm focal length lens. The straight dashed line shows complete transmission. The onset of the deviation from the linear behavior at 26 J/cm^2 is indicated as breakdown threshold. Other relevant values (Keldysh parameter γ = 1 and 0.5, self-focusing threshold) are also shown.

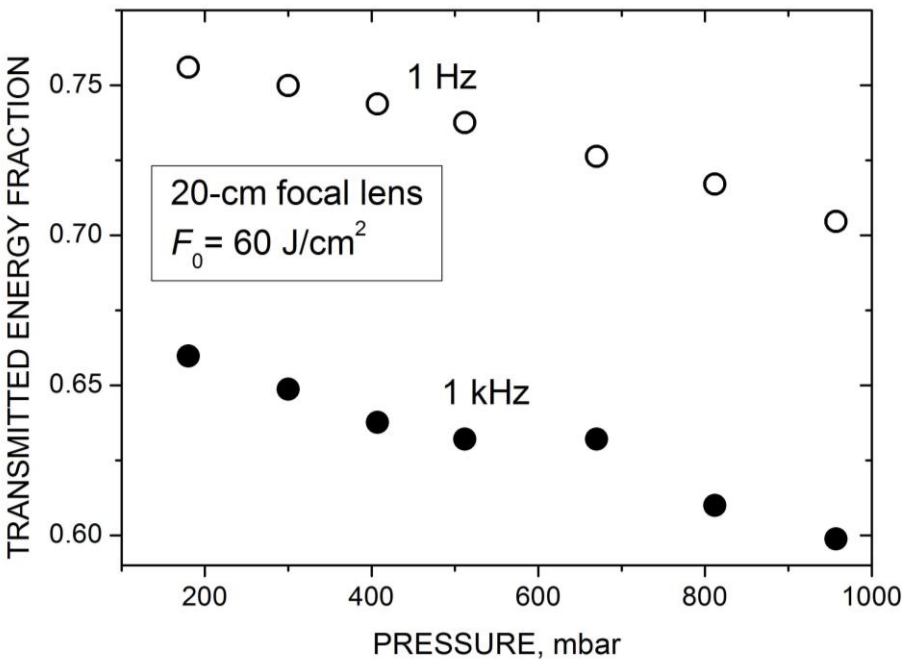

Figure 3. Transmitted laser pulse energy as a function of air pressure for different repetition rates.

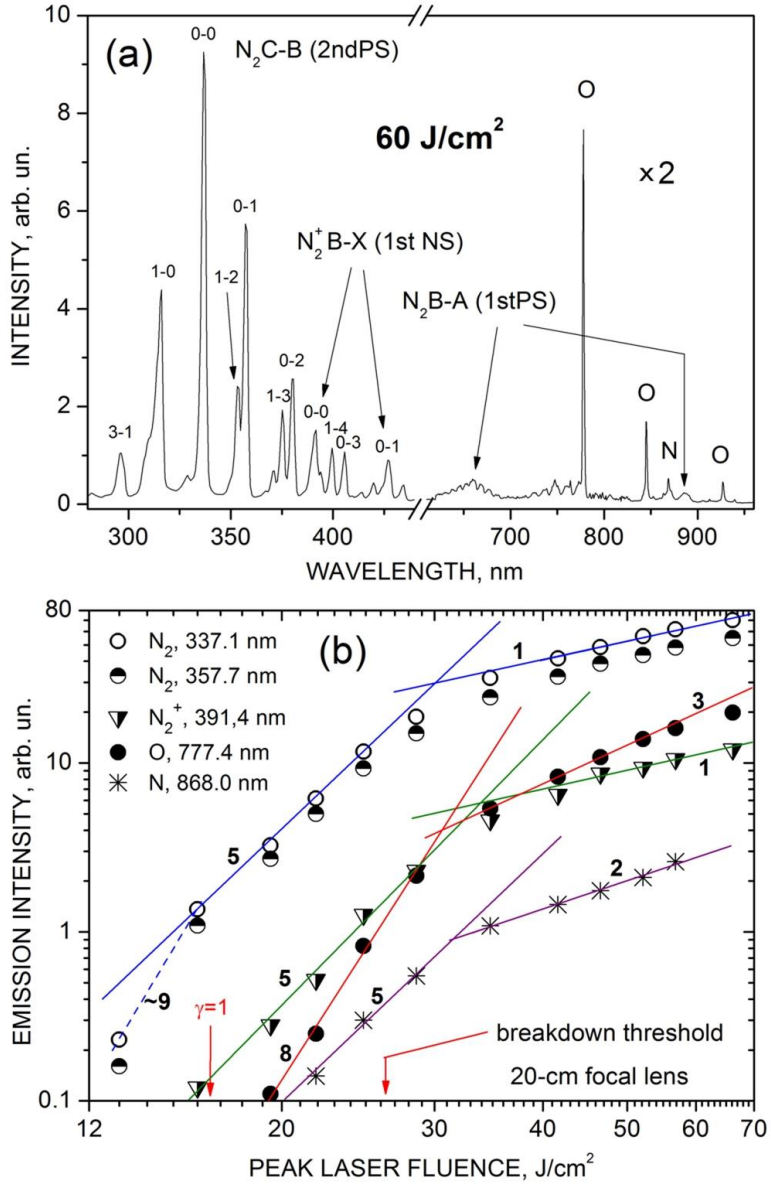

Figure 4. (a) Emission spectrum from the air focal region for input laser fluence of 60 J/cm^2. The pairs of numbers (v-v') above the peaks denote the vibrational levels of upper and lower electronic states of the transition. (b) Intensities I of some representative lines in the spectrum as a function of laser fluence F_0. The straight lines correspond to power-law fits $I \propto F_0^n$ with the exponent (slope) n shown near the corresponding line.

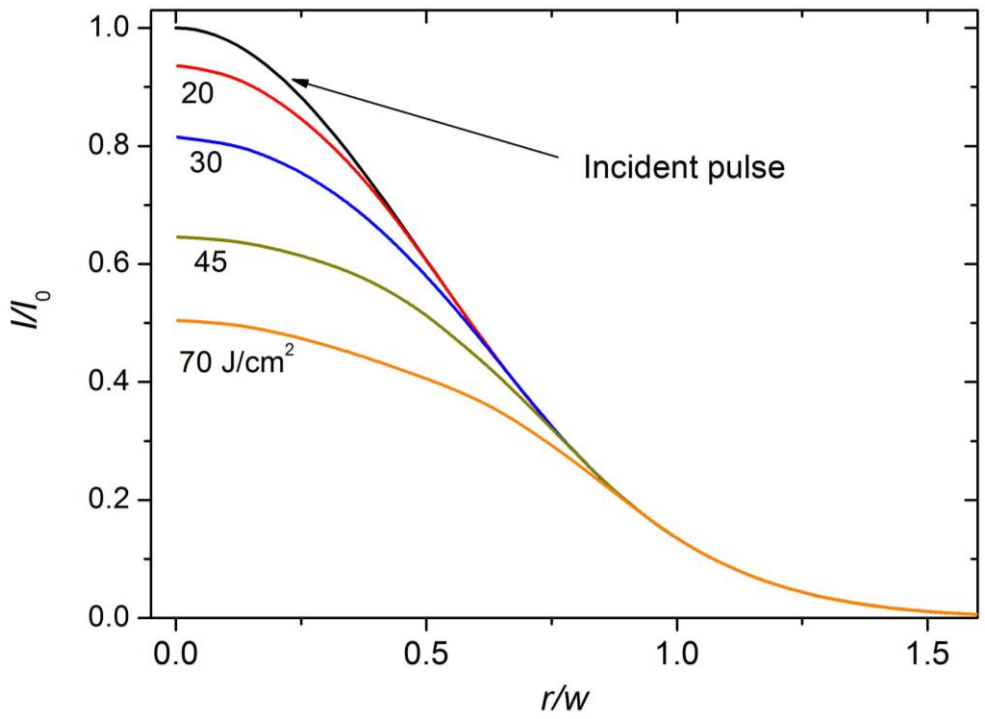

Figure 5. Calculated final profiles of the laser pulse after passing through the focal region for different input laser fluences (*w* is the $1/e^2$ radius of the beam at a distance after the focus where air ionization is negligible).